TISSUE ENGINEERING: Part C
Volume 17, Number 10, 2011

DOI: 10.1089/ten.tec.2011.0115

Development of Gellan Gum-Based Microparticles/ Hydrogel Matrices for Application in the Intervertebral Disc Regeneration

Diana Ribeiro Pereira, M.Sc.,[1,2] Joana Silva-Correia, Ph.D.,[1,2] Sofia Glória Caridade, M.Sc.,[1,2] Joao T. Oliveira, Ph.D.,[1,2] Rui A. Sousa, Ph.D.,[1,2] Antonio J. Salgado, Ph.D.,[2] Joaquim M. Oliveira, Ph.D.,[1,2] João F. Mano, Ph.D.,[1,2] Nuno Sousa, M.D., Ph.D.,[3] and Rui L. Reis, Ph.D.[1,2]

Low back pain is one of the most reported medical conditions associated to intervertebral disc (IVD) degeneration. Nucleus pulposus (NP) is often regarded as the structure where IVD degeneration begins. Gellan gum (GG)-based hydrogels for acellular and cellular tissue engineering strategies have been developed for finding applications as NP substitutes. The innovative strategy is based on the reinforcement of the hydrogel matrix with biocompatible and biodegradable GG microparticles (MPs), which are expected to improve the mechanical properties, while allowing to tailor its degradation rate. In this study, several GG MP/hydrogel disc formulations were prepared by means of mixing high acyl GG (0.75% (w/v)) and low acyl GG (2% (w/v)) GG aqueous solutions at different ratios, namely, 75%:25% (v/v), 50%:50% (v/v), and 25%:75% (v/v), respectively. The GG MP size was measured using a stereo microscope, and their dispersion within the hydrogel matrix was evaluated by means of staining the MPs with Toluidine Blue-O. The developed GG MPs/hydrogel discs were physicochemically characterized by Fourier-transform infrared spectroscopy and ^{1}H-nuclear magnetic resonance spectroscopy. The swelling behavior and degradation rate were assessed by immersion in a phosphate buffer saline for 14 days. The morphology and mechanical behavior were investigated by scanning electron microscopy and dynamic mechanical analysis, respectively. The mechanical properties of the hydrogel disc were improved by mixing the gels with the MPs. In addition, the possible cytotoxicity of the leachables released by MPs/hydrogel discs was screened *in vitro*, using a mouse lung fibroblast cell line (L929 cells). To investigate the encapsulation efficacy of L929 cells into the GG MPs/hydrogel discs, cells were stained with DAPI blue/Texas Red-Phalloidin and observed by confocal microscopy, after 24, 48, and 72 h of culturing. A cell viability assay was also performed using Calcein AM staining. The cell culture studies demonstrated that MPs/hydrogel discs are noncytotoxic over L929 cells. It was also demonstrated that L929 cells can be successfully encapsulated into the GG MPs of different formulations, remaining viable after 72 h of culturing. This study showed that GG hydrogel matrices reinforced with cell-loaded MPs could be a candidate strategy for NP regeneration.

Introduction

The tremendous increase in the number of patients suffering from low back pain (LBP) demands reliable clinical solutions urgently. Against a backdrop of intensive research, the consensus among how to best treat LBP still remains undefined.[1–3]

Human disability and suffering correlated with LBP is mainly caused by failure and degeneration of the intervertebral disc (IVD). The ability of the IVDs to move between spinal segments enables the spinal column to support dissimilar forces and massive loads.[4,5] Centrally situated into the IVD structure, nucleus pulposus (NP) is a gelatinous tissue surrounded by the annulus fibrosus (AF) on the radial periphery. These structures are sandwiched between two cartilaginous endplates, in both superior and inferior faces, which all together forms the IVD. After the age of 30, no blood vessels are present, which thus predisposes to IVD degeneration (IDD).[6] Concentric lamellae of AF are composed mainly by collagen type I and elastin radially organized, whereas the highly hydrated NP is primarily constituted by collagen type II.[7] The gel-like NP compartment contains

[1]3B's Research Group—Biomaterials, Biodegradables and Biomimetics, Headquarters of the European Institute of Excellence on Tissue Engineering and Regenerative Medicine, University of Minho, Guimarães, Portugal.
[2]ICVS/3B's—PT Government Associate Laboratory, Guimarães, Portugal.
[3]Life and Health Sciences Research Institute, School of Health Sciences, University of Minho, Braga, Portugal.

proteoglycans (PGs) such as versican, biglycan, decorin, fibromodulin, luminican, and especially aggrecan.[8] The limited IVD self-repair capacity results from the fact that nerves and blood vessels are mainly confined to AF. The environment around NP cells generally lacks nutrients, oxygen, glucose, and removal of waste products. Further, in the NP, cells are sparsely separated and are present in low number (5×10^3 cells/mm^3).[9] Disc-related pain is possibly associated with compression of the nerve route or irritation, stenosis and spondylolisthesis, and loss of disc weight.[10,11] The traditional medical therapies for treating chronic patients are contributing for increasing medical costs. Current treatments of IDD concern the relief of symptoms, mainly pain and do not underlie the associated biological NP changes. Monotherapies, such as well-defined pain-relieving pharmaceuticals, and traditional procedures to treat IVD disorders (e.g., bone fusion and discectomy) have been used, which have shown long-term ineffectiveness.[4] NP regeneration can be achieved following a tissue engineering (TE) strategy, which by definition proposes combination of biomaterials, cells, and bioactive molecules. This therapeutic strategy, should promote a natural repair process and restoration of healthy functions.[12,13] TE approaches are currently underway; still, it has not been possible to create a functional NP. This is mainly attributed both to incapacity to apply pressures mimicking the natural environment and insufficient knowledge of the complex IVD molecular functions.[14,15] Moreover, inadequate biomechanical behavior and integration of both new and native tissue are usually difficult to achieve.[12,16] The development of injectable systems that enables encapsulating cells and that mimics the NP biological and biomechanical characteristics has been attracting great deal of attention.[17,18] Hydrogels have been used for NP TE applications mainly due to its ability to swell and retain high amounts of water. Cell-based implants have been developed to promote *in situ* regeneration of NP by resembling its natural structure.[19–22] The combination of biological and biomechanical requirements have been addressed to restore the natural functions (i.e., physiological load distribution, and viscoelastic and transport properties) in a degenerated NP. Hydrogels (gel-like behavior) are promising materials to be used as IVD substitutes due to its similarity to the anatomic framework or extracellular matrix and hydrophilicity.[23] The use of a hydrogel as NP substitute is also advantageous, as it enables to be implanted using minimally invasive techniques, while restoring the disc volume. Moreover, hydrogels can be obtained using both nonharsh methods and reagents. The reinforcement of such hydrogels with microparticles (MPs) can improve the mechanical properties. Further, encapsulation of cells and/or biomolecules on MPs loaded on hydrogel matrices can enhance their biological performance. Nowadays, a variety of NP substitutes mimicking the native tissue have been synthesized from alginate,[24,25] collagen,[26,27] Gellan gum,[17,28] fibrin,[29] gelatin,[30] etc., to allow the formation of neo tissue.

Gellan gum (GG) is a polysaccharide derived by fermentation of bacterium *Spinghomonas elodea*, which has been proposed for TE strategies.[17,28,31–33] Two different types of GG are available: the acylated (high acyl Gellan gum, HAGG) and deacylated (low acyl Gellan gum, LAGG) forms. Both isoforms are composed of repetitive units of glucose, glucuronic acid, and rhamnose, including one carboxyl side group.[34] Both forms of GG are distinguishable concerning the gels they produce. HAGG originates soft, elastic, and nonbrittle gels, whereas LAGG produces hard, nonelastic, and brittle gels. The process of hydrogel formation procedure enables GG to assume a three-dimensional (3D) network structure.[23,35,36] At moderately high temperatures, GG chains are in a random-coil state, and by means of decreasing temperature, a transition from random-coil to double-helix occurs. After that, a structure made up of anti-parallel self-assembled double helices is formed producing oriented bundles called junctions zones. The untwined sites of the GG chains link the junction zones, thus originating a 3D framework. However, the gelation of such polysaccharide is strongly affected by the type and concentration of the ions, and thus these parameters should be considered when preparing GG hydrogels. Ionic-crosslinked hydrogels have a high mechanical stability due to the presence of multivalent, usually divalent, cations. The gelation in the presence of divalent cations allows the formation of more strongly crosslinked hydrogels than monovalent cations.[33,37,38]

MPs have been widely studied to engineer systems capable to deliver biomolecules, drugs, or cells.[39] To encapsulate living cells, different polymeric systems, for example, alginate spheres, have been proposed.[40] The noncytotoxicity, semi-permeability, and immune protection given by these systems allow to foresee their use in feasible approaches. Thus, the hydrogel matrix reinforced with MPs arises as a new approach for cell encapsulation, which also allows for the improvement of the mechanical properties.

In the present work, the main purpose concerned the development of a novel GG hydrogel system, consisting of GG MPs dispersed in a GG matrix, for finding application as an NP substitute in the regeneration of IVD. Several formulations of both GG forms (HAGG and LAGG) were prepared and gelation achieved by means of ionic-crosslinking using a phosphate-buffered saline (PBS, pH 7.4). The MPs processed were expected to improve the mechanical properties of the matrices. Therefore, mechanical behavior of the different formulations of GG MPs/hydrogel discs was investigated by dynamic mechanical analysis. The swelling behavior and degradation rate of the developed GG MPs/hydrogel discs were assessed by immersion in PBS (pH 7.4), over a period of 14 days. The possible cytotoxicity of the leachables released by the MPs/hydrogel discs was screened *in vitro* by means of using a mouse lung fibroblast cell line (L929 cells), after 72 h of culturing. Cell-loaded MPs/hydrogels were produced by preparing MPs loaded with cells, which were then incorporated into the different GG matrices. To qualitatively investigate the encapsulation efficacy of L929 cells into the GG MPs/hydrogel discs, a staining with DAPI blue/Texas Red-Phalloidin was performed, after 24, 48, and 72 h of culturing. A Live/Dead cell viability assay was also carried out (Calcein AM staining), followed by confocal microscopy observations.

Materials and Methods

Materials

LAGG (Gelzan™ CM) was purchased from Sigma-Aldrich and HAGG (KelcoGel LT100) from CP Kelco. Unless otherwise stated, all the reagents were purchased from Sigma-Aldrich.

GG MPs processing

Different formulations of GG MPs were obtained by means of combining 0.75% (w/v) HAGG and 2% (w/v) LAGG aqueous solutions at a ratio of 75%:25%, 50%:50%, and 25%:75% (v/v), respectively. GG solutions were prepared at room temperature. Each formulation was dissolved in distilled water at room temperature under constant stirring, for 24 h. To promote the complete dissolution of the powders, all solutions were agitated using an Ultra-turrax (Yellow Line DI 18B; Qlab) equipment, for 20 min.

Different GG MPs were produced by means of using a precision syringe pump (Fusion 200; Chemyx Inc.). A 1 mL syringe with an attached needle of 25G was filled with each GG formulation, and set in the syringe pump. A precipitation rate of 8 μL/min was used, and GG MPs were obtained by precipitation in a PBS (pH 7.4) solution, under agitation. Then, MPs were collected by filtration.

Preparation of the GG MPs/hydrogel matrices

Discs of the GG MPs/hydrogel for all three formulations were prepared by ionic-crosslinking in PBS. Each batch was composed by MPs and matrix, both obtained from the same formulation (i.e., 75%:25%, 50%:50%, or 25%:75% [v/v] HAGG:LAGG). Molds of silicone tube (height, 4 mm; diameter, 7 mm) were sterilized and filled with ~200 μL of the hydrogel previously mixed with MPs. Then, the molds were placed in a Petri dish and immersed in PBS to allow reticulation. As controls, discs without MPs were also prepared.

Physicochemical characterization of the LAGG and HAGG MPs/hydrogel matrices

Fourier-transform infrared spectroscopy. Fourier-transform infrared (FTIR) analysis was performed in HAGG and LAGG scaffolds using an IRPrestige-21 spectrometer (Shimadzu Corporation). The freeze-dried hydrogel discs were previously powdered and mixed with potassium bromide (KBr; Riedel-de Haën) to obtain transparent KBr pellets in the ratio of 1:10 of sample/KBr (w/w).[41] Then, the pellets were produced by uniaxially pressing the powders. Spectra were recorded in the range 4400–800 cm^{-1} using an average of 32 scans at a resolution of 2 cm^{-1}. The FTIR graphs were obtained using Origin Pro8 software (OriginLab).

^{1}H-nuclear magnetic resonance spectroscopy. ^{1}H-nuclear magnetic resonance (NMR) analysis was performed with a Varian Unity Plus spectrometer (equipped with a variable temperature system) operating at 300 MHz to investigate HAGG and LAGG chemical structures. The samples were prepared dissolving 10 mg of each freeze-dried hydrogel discs in 1 mL of deuterium oxide (D_2O), and the spectra were recorded at 70°C. The peak assigned at 4.3 ppm (D_2O) was used as reference. Graphic analysis of obtained data was performed using MestreNova software (Mestrelab Research).

MP size and distribution within the hydrogel matrices. The size of the GG MPs and distribution within the hydrogel matrices was investigated using a stereo microscope (Stemi 1000 PG-HITECH; Zeiss). GG MPs were observed before and after mixing with the hydrogel matrices. MPs alone were dispersed in a glass slide and observed under the stereo microscope. Each MPs image was obtained at 5× of magnification. The mean particle size was calculated in each provided image by measuring the diameter of each MP. The measurement of each MP was performed using the ImageJ software. To investigate the distribution of MPs within the hydrogel matrices, the MPs were stained with 1% (w/v) Toluidine Blue-O (Sigma) before incorporation into the hydrogel matrix. The hydrogel matrices loaded with the stained MPs were then observed under the stereo microscope.

Dynamic mechanical analysis. The viscoelastic measurements were performed using a TRITEC8000B DMA from Triton Technology equipped with the compressive mode, to characterize the mechanical behavior of different formulations of GG hydrogel discs (combining HAGG and LAGG). For Dynamic mechanical analysis (DMA), GG MPs/hydrogel matrices were produced incorporating 5, 50, or 500 mg/mL of MPs. The measurements were carried out at 37°C. Samples with cylindrical shapes around 7 mm diameter and 4 mm thickness were produced accurately for each sample. The different GG MPs/hydrogel and GG hydrogel discs were analyzed by immersion in a liquid bath contained in a Teflon® reservoir. The geometry of the samples was then measured, clamped in the DMA apparatus, and immersed in the PBS. After equilibration at 37°C, the DMA spectra were acquired during a frequency scan between 0.1 and 10 Hz. The experiments were performed under constant strain amplitude (50 μm). A small preload was applied to each sample to ensure that the entire scaffold surface was in contact with the compression plates before testing. For all scaffolds being tested, the distance between plates was equal. The DMA analysis was performed in three samples for each condition.

Swelling behavior and degradation study. For swelling and degradation studies, 50 mg/mL of MPs was incorporated into the hydrogel matrices. The hydrogels' swelling ability was investigated by means of soaking the lyophilized GG hydrogel discs ($n = 3$) in PBS. This study was performed at 37°C under constant shaking (60 rpm) for 15 days. The swelling ability of each hydrogel formulation was calculated based on the changes of the initial dry mass (m_i), after incubation in PBS. Swollen hydrogel discs were removed from PBS, and analyzed at different time points. The excess of fluid was eliminated using a filter paper and the wet mass (m_w) weighted using an analytical balance. After that, the scaffolds were frozen at −80°C and freeze-dried. After freeze-drying, the scaffolds were weighted and the final dry mass was determined (m_d) to calculate weight loss. To determine the percentage of water uptake of the scaffold (WUs) after each time point (t), and the percentage of weight loss of the scaffold (WLs) after each time point (t), Equations (1) and (2) were applied, respectively:

$$\mathrm{WUs, t}(\%) = [(m_{w,t} - m_i)/m_i] \times 100 \quad (1)$$

$$\mathrm{WLs, t}(\%) = [(m_i - m_{d,t})/m_i] \times 100 \quad (2)$$

The studies were performed using three samples per experimental condition ($n = 3$).

Scanning electron microscopy. All formulations of the GG hydrogel discs were frozen at −80°C after production,

and freeze-dried to investigate their morphology. Before observation, the specimens were sputter coated with a mixture of gold-palladium. A Nova NanoSEM 200 microscope (FEI) with an attached energy dispersive spectrometer (Pegasus X4M) was used. The equipment was operated at an accelerating voltage of 5 kV, and images were captured at 200×, 1000×, and 10,000× of magnification.

In vitro *studies*

Two-dimensional *in vitro* studies: screening cytotoxicity (MTS assay). The cytotoxicity of the different GG hydrogel matrices, with or without MPs, was assessed using an immortalized mouse lung fibroblasts cell line (L929) purchased from European Collection of Cell Cultures (ECACC). The effect of the leachables released from the materials (within a 24 h extraction period) on cellular metabolism was performed using a standard MTS (3-(4,5-dimethylthiazol-2-yl)-5(3-carboxymethoxyphenyl)-2(4-sulfofenyl)-2H-tetrazolium) (Cell Titer 96® Aqueous Solution Cell Proliferation Assay; Promega) viability test in accordance with ISO/EN 10993 part 5 guidelines.[42] This assay was performed to investigate the possible cytotoxicity of the several GG hydrogel matrices. This assay is based on the bioreduction of the substrate (MTS) that is converted into a brown formazan product by metabolically active cells, specifically, in presence of dehydrogenase enzymes.[43] The GG matrices, with or without MPs, were produced as aforementioned, under sterile conditions. A minimum of 4 g of each material was incubated for 24 h in 20 mL of complete Dulbecco's modified Eagle's medium (DMEM; Sigma) in a thermostatic bath (37°C) with constant shaking (60 rpm) to produce the extracts. A latex rubber extract was used as positive control for cell death, and complete culture medium was used as negative control representing the ideal situation for cell proliferation. The cells were grown in monolayer in DMEM culture medium supplemented with 10% fetal bovine serum (FBS, heat-inactivated; Biochrom) and 1% of an antibiotic–antimycotic mixture (Invitrogen). A chemical method using trypsin (0.25% trypsin-EDTA solution; Sigma) was used to promote cell detachment from the culture flasks. L929 cells seeded at a density of 1×10^5 cells/well into a 48-well plate (200 μL/well) were incubated for 24 h at 37°C in a humidified atmosphere of 5% CO_2. After that, culture medium was replaced with 200 μL of each extraction fluid. The MTS assay was performed after culturing the cells in the presence of the extraction fluids for 24, 48, and 72 h, under standard culture conditions. A mixture of serum-free culture medium without phenol red and MTS (CellTiter 96 One Solution Cell Proliferation Assay Kit; Promega) was put in contact with the cells.

The optical density (OD) was measured at 490 nm in a microplate reader (Molecular Devices) with $n=4$, two independent times. The percentage of cell viability was calculated after normalization with the mean OD value obtained for the negative control.

3D *in vitro* studies: Cell-loaded GG MPs/hydrogel matrices (constructs). To obtain the cell-loaded MP/hydrogel matrices, an immortalized mouse lung fibroblast cell line (L929) purchased from European Collection of Cell Cultures (ECACC) was first encapsulated into the GG MPs. L929 cells were grown in monolayer in complete DMEM culture medium (Sigma) supplemented with 10% FBS (heat-inactivated; Biochrom) and 1% of an antibiotic–antimycotic solution (Invitrogen). A chemical method using trypsin (0.25% trypsin-EDTA solution; Sigma) was used to promote cell detachment from the culture flasks, after the cells have reached confluency. A cell suspension containing 2.5×10^6 cells/mL was prepared, and then centrifuged at 1200 rpm for 5 min. Afterward, the culture medium was completely aspirated, and the cell pellet was re-suspended in each GG hydrogel formulation, using a volume of 1 mL. The mixture of cells and hydrogels was centrifuged at 600 rpm for 3 min to promote cells homogenization. Then, a 1 mL syringe was filled with each hydrogel formulation (cells + hydrogels). To process standardized MPs, each MPs batch was produced at 50 μL/min rate. The rate used to precipitate MPs was increased in the cellular approach to accelerate the process, avoiding cell damage or even death. Different formulations of MPs loaded with L929 cells were obtained by precipitation in PBS, and equilibrated for 30 min. Then, the MPs were collected for further incorporation within the hydrogel discs as previously described.

Confocal microscopy (DAPI/TEXAS RED-PHALLOIDIN staining). Confocal microscopy was performed to obtain 3D images of the cells distributed within the GG MPs/hydrogels matrices. Images were acquired using an Olympus Fluoview 1000 confocal microscope (Olympus).

After different times of culturing in standard conditions, the culture medium was aspirated and the cell-loaded GG MPs/hydrogel matrices were collected. Afterward, the samples were stained with 4,6-Diamidino-2-phenyindole, dilactate (DAPI; Sigma). The DAPI solution was removed, and the same hydrogels were stained with Phalloidin-Tetramethylrhodamine B isothiocyanate (Texas Red-Phalloidin; Sigma). The software FV10-ASW 2.0 Viewer was used to provide confocal images and videos (provided as Supplementary Data; Supplementary Data are available online at www.liebertonline.com/tec).

Inverted microscopy (CALCEIN AM staining). After each period of culturing in standard conditions, cell viability was assessed by staining the cell-loaded GG MPs/hydrogel matrices with Calcein AM (Molecular Probes). Briefly, the constructs were incubated in DMEM without phenol red for 24, 48, and 72 h. After each culture period, the constructs were stained by adding 2 μL of Calcein AM and 1 mL of DMEM without phenol red. To allow membrane permeation, the constructs were incubated for 10 min. The green fluorescence was observed in an Olympus IX81 inverted microscope (Olympus). The images of Calcein AM staining were analyzed using the cell^B basic imaging software (Olympus).

Statistical analysis. Statistical analysis (GraphPad Prism; GraphPad Software) concerning the MTS assay was performed using one-way analysis of variance followed by Tukey's post-test with a significance set at $p<0.05$. The data on the MPs size were analyzed using Student's *t*-test with a statistical significance set at $p<0.05$. All results are presented as the mean ± standard deviation.

Results

In this study, different formulations for processing GG-based MPs (MPs)/hydrogel matrices were produced com-

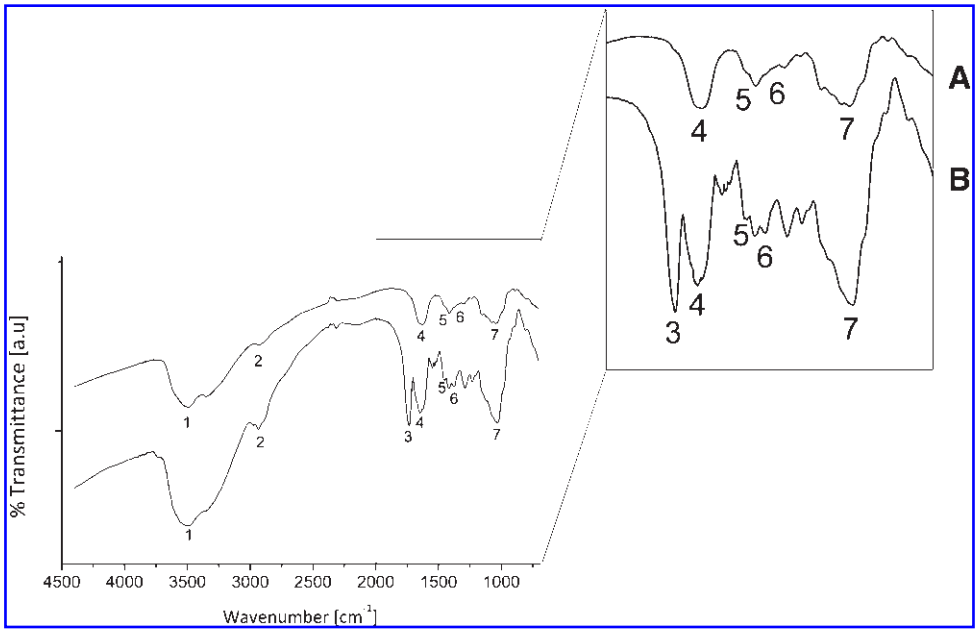

FIG. 1. Fourier-transform infrared spectra of **(A)** High acyl Gellan gum (HAGG) and **(B)** Low acyl Gellan gum (LAGG) powders. The peak at 1748 cm^{-1} is assigned to the C-O stretching of acyl group at HAGG. Peaks assignment is shown in Table 1.

bining LAGG and HAGG. HAGG and LAGG solutions were mixed at different ratios (75%:25%, 50%:50%, and 25%:75% [v/v] HAGG:LAGG). MPs were obtained from these formulations by using a syringe pump for precipitation in PBS. To preserve the molecular structure of both GG forms, the method was temperature independent; that is, the solutions did not need to be heated to allow the complete dissolution of the powders as it was proposed in the work performed by Oliveira *et al.*[33] Instead, we used an Ultra-turrax equipment to facilitate the dissolution of both forms of GG. Both MPs and GG MPs/hydrogel matrices were equilibrated in PBS for inducing the ionic-crosslinking of the hydrogels.

Physicochemical characterization of the LAGG and HAGG MPs/hydrogel matrices

The physicochemical analysis of all GG MPs/hydrogel matrices was assessed by using different characterization techniques. FTIR spectroscopy is used to identify the presence and the environment of functional groups in organic molecules. It is the simplest and most reliable method to obtain the characteristic absorption bands of functional groups. The typical bands of GG were present in both forms (HAGG and LAGG) at 3473 cm^{-1}, 2920 cm^{-1}, 1618 cm^{-1}, 1536 cm^{-1}, 1412 cm^{-1}, and 1037 cm^{-1} (Fig. 1 and Table 1). To confirm the presence of the acyl groups in HAGG, GG samples were analyzed by ^{1}H NMR spectroscopy (Fig. 2). The chemical shift for both forms has revealed characteristics peaks at 5.15, 1.32, 4.73, and 4.55 ppm. In addition, the HAGG spectra also revealed a peak at 2.19 ppm.

The MPs were produced in an automated drop-by-drop system, that is, a syringe pump. Macroscopically, it was possible to observe that the particle size did not varied significantly for the different hydrogel formulations (Table 2). From Figure 3, it was possible to observe that MPs present a tear shape. The quantity of MPs incorporated into the hydrogel matrices could represent a factor of stability/instability; therefore, MPs quantification should be considered to assure the total integrity and cohesion of the structure. To better understand the performance of the hydrogels reinforced with MPs, three different approaches were considered for each formulation. Different quantities of MPs were used to reinforce the GG hydrogel matrices: 5, 50, and 500 mg/mL. It was possible to verify macroscopically the nonintegrity of the hydrogels reinforced with MPs at a concentration of 500 mg/mL. The matrix was not surrounding the MPs and some of them were found in PBS a few hours

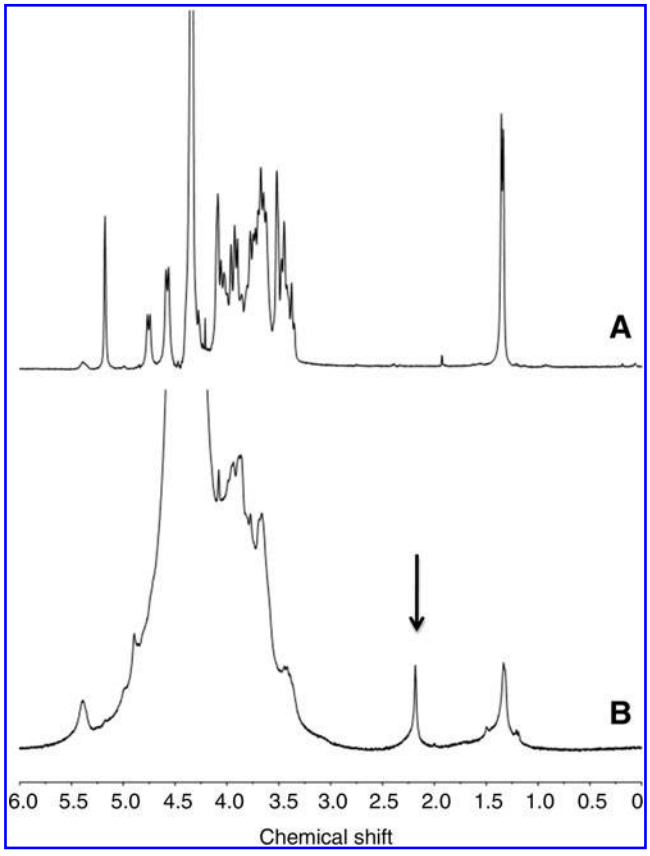

FIG. 2. ^{1}H-nuclear magnetic resonance spectra of **(A)** LAGG and **(B)** HAGG.

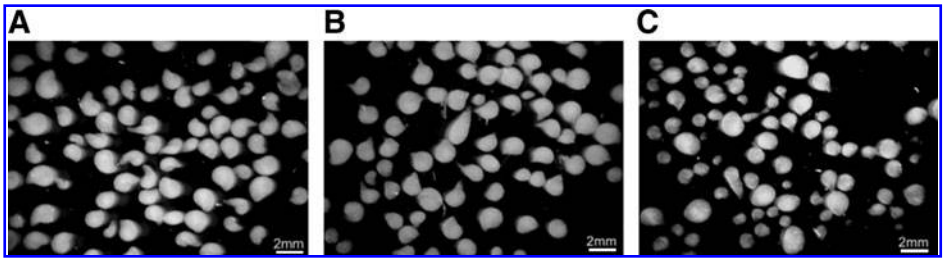

FIG. 3. Macroscopic images of the microparticle (MP) size made up by different formulations: **(A)** 75% HAGG:25% LAGG, **(B)** 50% HAGG:50% LAGG, and **(C)** 25% HAGG:75% LAGG. The MP size is shown in Table 2.

after being processed, which revealed a poor cohesion of the MPs within the hydrogel matrix. Figure 4 shows the incorporation of 50 mg/mL of MPs within the hydrogel matrix. The MPs were previously stained with Toluidine Blue-O at a concentration of 1% (w/v), and then incorporated into the hydrogel matrix. As it can be observed in Figure 4, the MPs incorporated into the hydrogel discs were sparsely distributed.

Dynamic mechanical analysis (DMA) was performed to study the effect of the incorporation of the MPs within the GG hydrogel matrices (Fig. 5). The DMA analyses were performed on samples in the wet state, and in a hydrated environment (PBS). The mechanical behavior was assessed throughout a physiological relevant frequency range (0.1–10 Hz). The reinforcement of GG hydrogel matrices with GG MPs was evaluated by using three different quantities of MPs: 5, 50, and 500 mg/mL of MPs were incorporated to each hydrogel formulation. LAGG hydrogel matrices at 2% (w/v) and hydrogel matrices of each formulation without MPs were used as controls.

To evaluate the water uptake ability and weight loss of the GG MPs/hydrogel matrices, *in vitro* studies were performed in PBS for 14 days (Fig. 6). In Figure 6A, the capacity of GG hydrogel matrices to absorb water is presented. Regarding these results, the hydrogel matrices comprising 50% HAGG:50% LAGG (v/v) have shown a significantly higher water uptake ability than the other formulations. Actually, the water uptake ability of the GG hydrogels after 14 days ranged from 2000% up to ~4000%. Figure 6B shows the weight loss of the different GG formulations. From this figure, it is possible to observe a similar behavior for all the GG hydrogel matrices. However, the GG hydrogel matrices comprising 75% HAGG:25% LAGG (v/v), with and without MPs reinforcement, have revealed a significantly higher degradation as compared to the other formulations.

The morphology of the freeze-dried GG hydrogel matrices was assessed under scanning electron microscopy (SEM) (Fig. 7). A highly porous 3D sponge-like morphology was observed in the cross-sectional images of all discs. However, there was an increase in pore size by means of increasing the percentage (v/v) of LAGG at 2% (w/v) in the formulations. From the SEM images corresponding to LAGG and HAGG (Fig. 7D and E, respectively), it is possible to observe that pore size and quantity are completely different. Freeze-dried LAGG formulation presents larger pores, whereas HAGG possesses many pores of smaller diameter.

Two-dimensional in vitro *studies: Screening cytotoxicity (MTS assay)*

Different assays can be performed to assess the cytotoxicity *in vitro*. An immortalized mouse lung fibroblast cell line (L929 cells) was used to preliminarily screen the possible cytotoxicity of the materials.[42] All the GG hydrogel formulations showed no significant differences as compared to the negative control (Fig. 8).

In vitro *3D study: Cell-loaded GG MP/hydrogel matrices (constructs)*

The constructs were stained with DAPI blue (nucleus staining) and Texas Red-Phalloidin (cytoskeleton staining) to verify the efficiency of the encapsulation process. From the confocal microscopy images shown in Figure 9, it is possible to confirm the presence of cells loaded into the MPs in all formulations. MPs delimitation was not possible to observe since the MPs were integrated in a hydrogel matrix obtained from the same formulation. Despite, a round shape formed by the stained cells was observed, which indicates that cells are confined to the MPs. Moreover, although the cells were present in the MPs at different time points, the quantity of cells did not rise up throughout the time.

To assess cell viability, cell-loaded MPs/hydrogel matrices were stained with Calcein AM. This compound is able to permeate the plasma membrane and be converted into Calcein by metabolically active cells. The cleavage of such fluorochrome by intracellular esterases results in the emission of green fluorescence that can be observed under a fluorescence microscopy apparatus.[44] Calcein AM assay was performed at different time points of culture (Fig. 10). In all

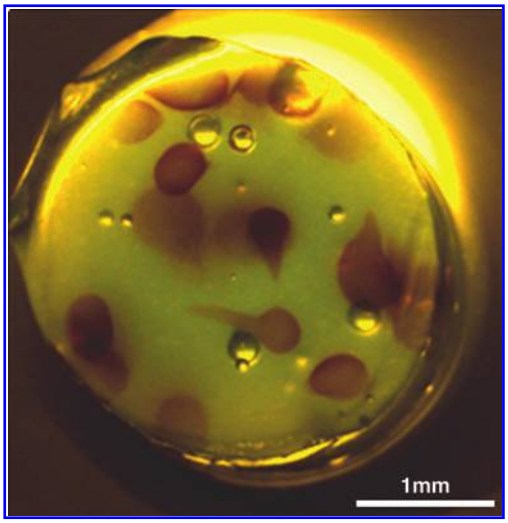

FIG. 4. Typical image of the GG MP/hydrogel discs. Dispersion of MP at a concentration of 50 mg/mL within the GG-hydrogel discs. MPs were stained with Toluidine Blue-O before being mixed with the GG matrix. GG, Gellan gum; MP, microparticles. Color images available online at www.liebertonline.com/tec

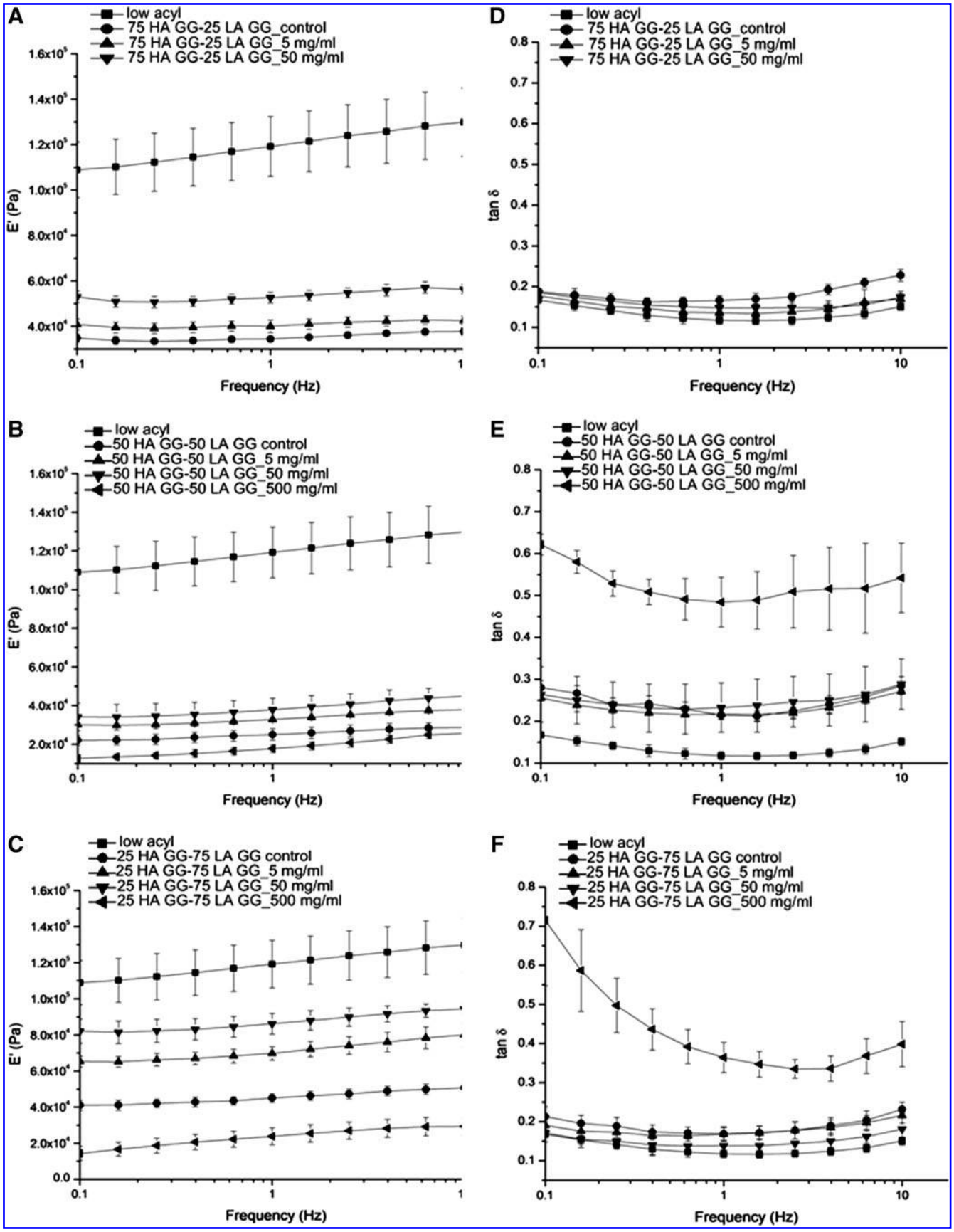

FIG. 5. Dynamic mechanical analysis of GG-based hydrogel/matrices made up by different formulations: **(A–C)** graphs corresponding to storage modulus (E′): 75% HAGG:25% LAGG, 50% HAGG:50% LAGG, and 25% HAGG:75% LAGG, respectively and **(D–F)** graphs corresponding to loss factor (tan δ): 75% HAGG:25% LAGG, 50% HAGG:50% LAGG, and 25% HAGG:75% LAGG, respectively.

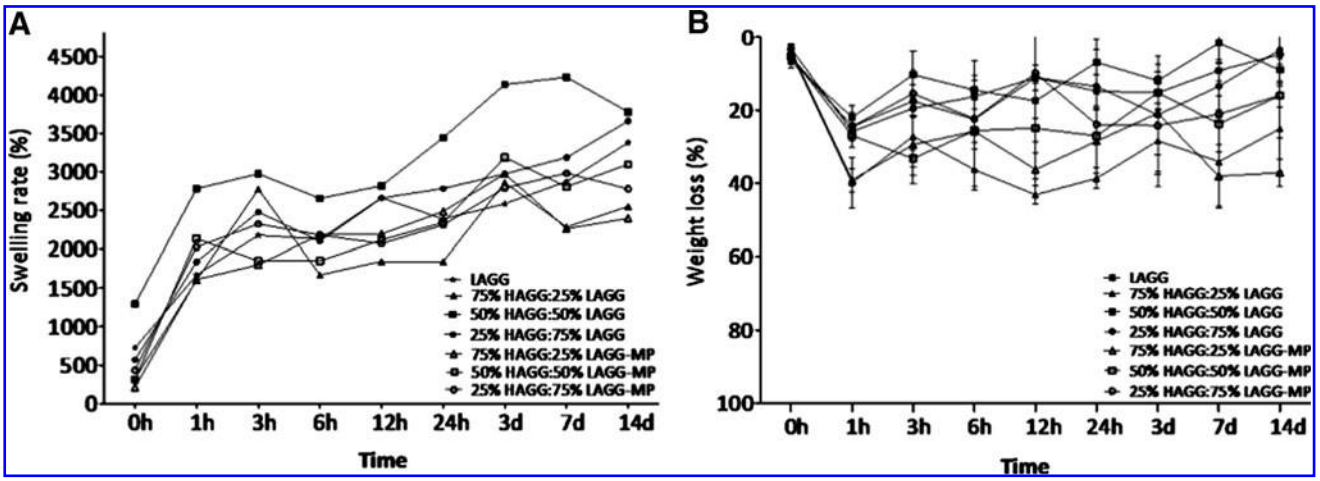

FIG. 6. **(A)** Water uptake and **(B)** weight loss of different GG formulations: LAGG 2%; 75% HAGG:25% LAGG, 50% HAGG:50% LAGG, 25% HAGG:75% LAGG, 75% HAGG:25% LAGG (50 mg/mL MPs); 50% HAGG:50% LAGG (50 mg/mL MPs), and 25% HAGG:75% LAGG (50 mg/mL MPs).

formulations, positive results (green fluorescence) were obtained at different time points, which indicate that cells are alive.

Discussion

The use of different GG forms for developing hydrogel substitutes to NP regeneration presents the advantage of enabling to be implanted using minimally invasive techniques. The combination of LAGG and HAGG was performed with the rationale that HAGG could allow the tailoring of hydrogel degradation rate, as well as the improvement of cellular metabolic activity. Moreover, the incorporation of MPs in the GG hydrogels is expected to improve their mechanical properties. The mild conditions used to obtain the hydrogel formulations were considered an important modification of the previous method,[31–33] avoiding the heating of the solutions at high temperatures, which can be deleterious for cell encapsulation and viability. So, in this study, cell encapsulation was performed by means of dissolving GG at room temperature, thus avoiding cell damage or even death. Despite, there is the need to carry out further studies to elucidate the influence of hydrogel temperature on cells viability during the encapsulation step. To our knowledge, the reinforcement of such hydrogel matrices with MPs is herein proposed for the first time, and aims to improve the mechanical properties of the hydrogel systems, while allowing cells encapsulation in mild conditions.

Physicochemical characterization of the LAGG and HAGG MPs/hydrogel matrices

In this work, LAGG and HAGG were first physicochemically characterized by FTIR. The degree of acylation is directly related with the properties of the GG hydrogel. The native form of GG (HAGG) implies a critical control of the structure and it can presents some purity issues.[38] The absorption band at 1618 cm^{-1} corresponds to the glycosidic bond in GG (LAGG and HAGG).[41] In the FTIR spectra of HAGG, it was observed a peak at 1748 cm^{-1}, which did not

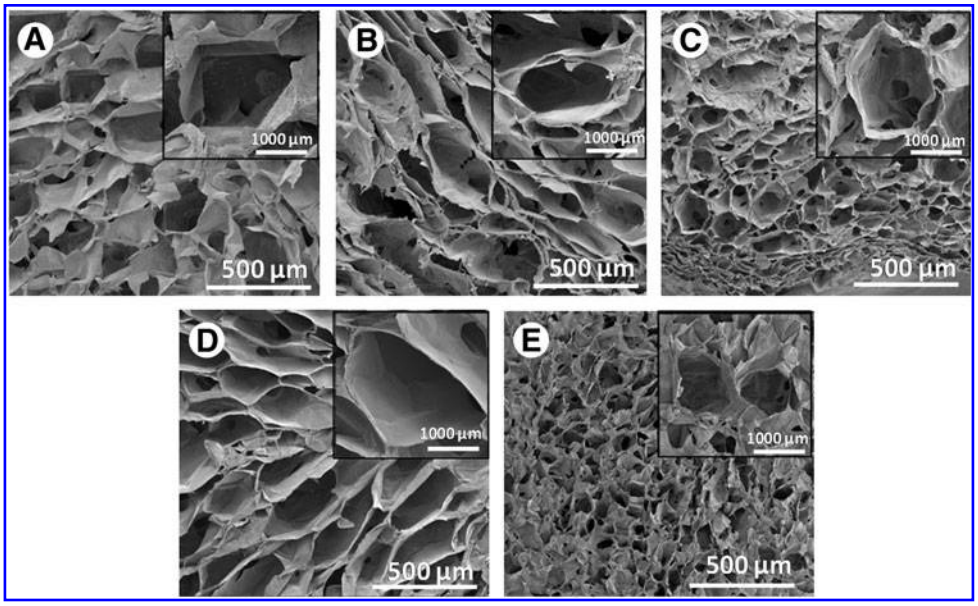

FIG. 7. Scanning electron microscopy images of the freeze-dried GG hydrogel formulations: **(A)** 25% HAGG:75% LAGG, **(B)** 50% HAGG:50% LAGG, **(C)** 75% HAGG:25% LAGG, **(D)** LAGG 2%, and **(E)** HAGG 0.75%.

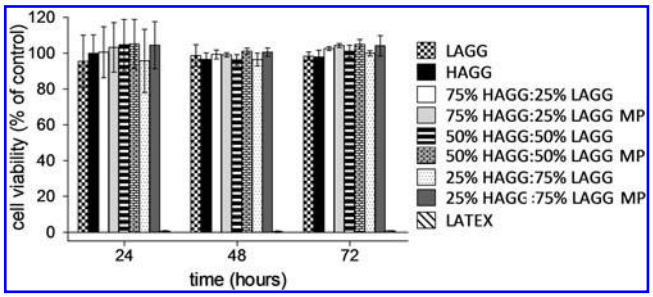

FIG. 8. Cytotoxicity screening of the different formulations of the different formulations of GG hydrogel with or without MP leachables using rat lung fibroblasts (L929 cells). Latex extract (Latex) and standard culture medium were used as positive and negative controls, respectively. An MTS assay was performed after 24, 48, and 72 h.

appeared in LAGG spectra (Table 1). This is a characteristic peak of the acyl group, which is present in the molecular structure of HAGG.

The acyl groups integrating the HAGG structure were also verified through analysis of ^{1}H NMR spectra. The chemical shift for LAGG and HAGG has revealed characteristic peaks at 5.15 and 1.32 ppm, assigned to H-1 and H-6 of the α-anomers of L-rhamnopyranosyl residue.[45] Moreover, signals at 4.73 and 4.55 ppm, corresponding to D-glucopyranosyl and D-glucopyranosyl residues, respectively, were observed in both ^{1}H NMR spectra. In addition, the HAGG spectra revealed a peak at 2.19 ppm, which should be attributed to the acyl groups of HAGG.[45]

The shape in the form of a tear presented by the MPs can be attributed to the processing method (i.e., using a syringe pump) and to the high viscosity of the hydrogel formulations. The size of MPs is an important feature when considering their use in encapsulating processes. The size kept at "micro" scale is optimal for allowing the encapsulation of cells. However, a statistically significant difference was found between the dimensions of the MPs of the different formulations. The significant differences observed can be related with the high viscosity of the formulation, which varies according to the percentage of HAGG and LAGG. However, it is possible to conclude about the feasibility of this method to obtain MPs in a standard way. The hydrogel matrices reinforced with MPs should exhibit total construct integrity. Nevertheless, the quantity of MPs reinforcing the hydrogels is an important feature to develop suitable MPs/hydrogel matrices. Moreover, the dispersion of such MPs inside the hydrogel matrix is also critical: they might be sparsely distributed, to avoid different properties in respect to both mechanical and biological performance.

The reinforcement of hydrogels matrices with cell-loaded MPs should tackle some requirements: matrices should exhibit a suitable mechanical and biological behavior and preferentially resemble the native NP.

Succinctly, DMA analysis revealed that the storage modulus of all hydrogel formulations increased by means of increasing frequency. However, the behavior of the hydrogels resembled a viscoelastic material in contrast to the human IVD, which reveals a linear viscoelasticity during compression.[46] However, Leahy and Hukins[47] have reported a similar increase in the storage modulus of a sheep model. Silva-Correia *et al.*[17] reported a storage modulus of 89.5 ± 7.4 kPa for ionic-crosslinked methacrylated GG (GG-MA) hydrogels. Regarding the loss factor of those hydrogels the values were around 0.15 and 0.21 at 1 Hz. A new approach based on GG hydrogels was used throughout the reinforcement of the hydrogels with MPs. Through analysis of DMA data, it was possible to observe the efficient reinforcement produced by 50 mg/mL of MPs in all GG MPs/hydrogel matrices. From those results, the formulation of 25% HAGG:75% LAGG (v/v) presented a better performance as compared to the other

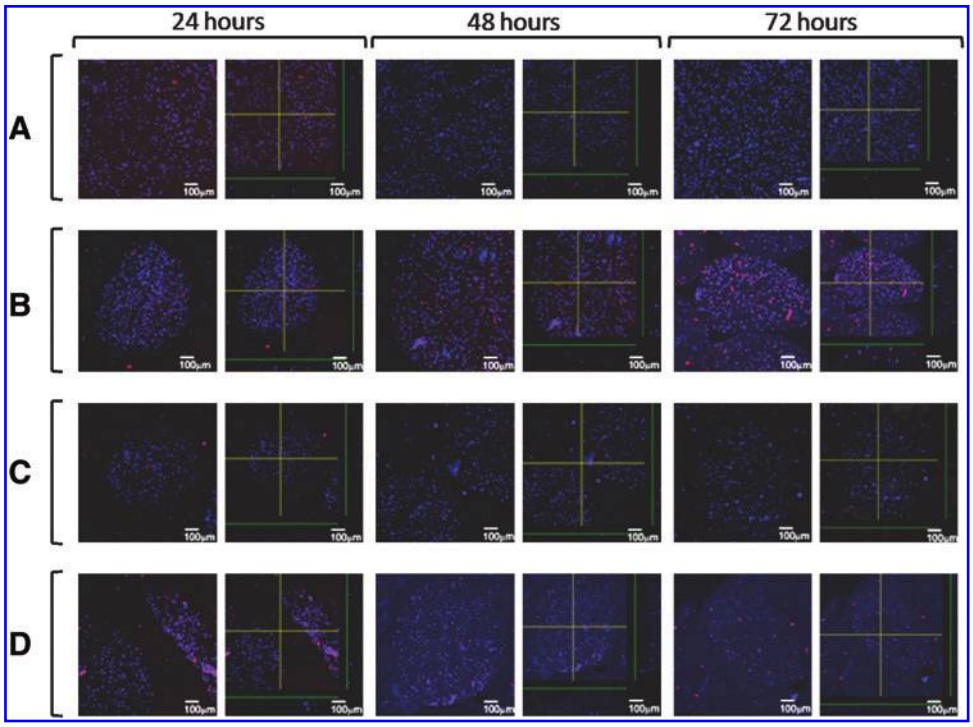

FIG. 9. Confocal microscopy images of the L929 cells encapsulated within the different GG MPs loaded into GG discs: **(A)** LAGG 2%, **(B)** 75% HAGG:25% LAGG (50 mg/mL MPs), **(C)** 50% HAGG:50% LAGG (50 mg/mL MPs), and **(D)** 25% HAGG:75% LAGG (50 mg/mL). All the GG MPs/hydrogel matrices were cultured for 24 until 72 h (blue color [DAPI blue] corresponds to cells nuclei; red color [Tex Red Phalloidin] is attributed to the stained cells cytoskeleton). Color images available online at www.liebertonline.com/tec

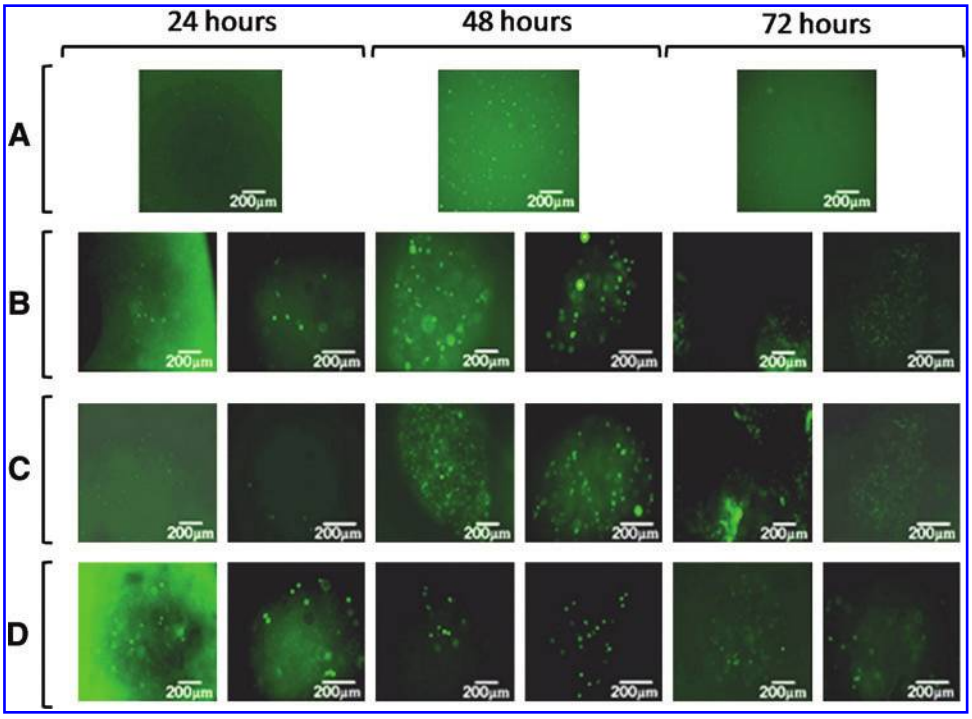

FIG. 10. Images of the L929 cells encapsulated within different GG MPs loaded into GG discs: **(A)** LAGG 2%, **(B)** 75% HAGG:25% LAGG (50 mg/mL MPs), **(C)** 50% HAGG:50% LAGG (50 mg/mL MPs), and **(D)** 25% HAGG:75% LAGG (50 mg/mL MPs). The loaded discs were stained with Calcein-AM, and cultured for 24 until 72 h. Color images available online at www.liebertonline.com/tec

formulations in respect to mechanical properties. The storage modulus at 1 Hz for 75% HAGG:25% LAGG (v/v) (52.7 ± 2.33 kPa), 50% HAGG:50% LAGG (v/v) (37.9 ± 5.9 kPa), and 25% HAGG:75% LAGG (v/v) (86.2 ± 5.75 kPa) corresponding to an incorporation of 50 mg/mL of MPs demonstrated the efficacy in improving the mechanical properties of the matrices. In fact, it was also seen that the mechanical properties of the GG hydrogels were lower when no MPs were incorporated into the gels or when MPs are mixed at a final concentration of 5 and 500 mg/mL. The GG MPs/hydrogel matrices made using the formulation 25% HAGG:75% LAGG (v/v) reinforced with 50 mg/mL of MPs have revealed values for the storage modulus identical to the ones obtained for GG-MA.[17] However, no GG formulation previously reported elsewhere performed better than LAGG at 2% (119.2 ± 13.2 kPa). The optimal outcome to reinforce GG matrices may be in the range of 50–500 mg/mL of incorporated MPs. However, the concentration of 500 mg/mL of MPs to reinforce the matrices is, in our point of view, extremely high to promote the reinforcement, since during our studies it was possible to verify that MPs were already dispersed in PBS, before analysis. This fact demonstrated that the GG MPs/hydrogel matrices reinforced with 500 mg/mL have shown noncohesion and loss of integrity. The loss factor (tan δ) is often considered as a measure of damping capability of the material. In all formulations incorporated with 500 mg/mL of MPs, it was also possible to verify the low damping properties of those GG MPs/hydrogel matrices. The incorporation of a viscoelastic material (MPs) within another viscoelastic material (matrix) changed the loss factor for undesired values. LAGG at 2% (w/v) showed the better damping behavior among all gels, with values of 0.12 ± 0.0099. The reinforcement of the formulations with 5 and 50 mg/mL showed a relatively similar behavior, with loss factor values comprised between 0.1 and 0.2.

The data resulting from swelling and degradation studies showed that it is possible to tailor both water uptake and weight loss by means of using different ratios of HAGG and LAGG. Regarding the degradation studies, the higher degradation shown by GG hydrogel matrices composed of 75% HAGG:25% LAGG (v/v) can be related with the pore size (Fig. 7). In fact, the SEM images of freeze-dried scaffolds comprising 75% HAGG:25% LAGG (v/v) revealed pores possessing a lower pore diameter as compared to others. Thus, it can be stated that it is possible to adjust the degradation rate of these hydrogels by using different ratios of HAGG and LAGG.

Two-dimensional in vitro *studies: Screening cytotoxicity*

A L929 cell line was used to screen the possible cytotoxicity of the leachables released by the developed GG hydrogels. The results showed that for all the periods tested, the L929 cells remained metabolically active after contacting with the different extract fluids. All the materials have shown no statistical differences as compared to the negative control, and therefore it is possible to state that these GG formulations are noncytotoxic over L929 cells. According to what was expected, a clear toxic effect on cell viability was produced by latex (positive control for cell death).

Table 1. Peak Assignment of the Characteristic Bands Revealed by Fourier-Transform Infrared Spectra of High Acyl Gellan Gum and Low Acyl Gellan Gum Powders

Peak	(cm^{-1})	*Assignment*
1	3420	O-H stretching peak
2	2920	C-H stretching
3	1748	C-O stretching
4	1618	Asymmetric COO- stretching
5	1536	C-C stretching
6	1412	Symmetric COO- stretching
7	1037	C-O stretching

Table 2. Microparticles Mean Size of All Formulations

MP formulation	*MP number*	*MP size (mean ± SD)*
75% HAGG:25% LAGG	76	671 ± 143 μm
50% HAGG:50% LAGG	80	741 ± 127 μm
25% HAGG:75% LAGG	71	580 ± 143 μm

MP, microparticle; HAGG, high acyl Gellan gum; LAGG, low acyl Gellan gum.

In vitro *3D study: Cell-loaded GG MP/hydrogel matrices*

A 3D network reported for alginate beads is able to preserve the cells phenotype, leading to normal performance of cells without changes at the cellular and molecular level.[22] Thus, to conclude on which is the best GG formulation to encapsulate cells, we carried out complementary *in vitro* studies. The presence of acyl groups in HAGG is expected to improve the biological performance, so it is likely that formulations with higher percentage of HAGG could enhance the biological behavior. By performing the nuclei staining, we were not able to conclude on the cells viability. To circumvent this issue, a Calcein AM assay was performed. As it was shown in Calcein AM images, a concentric cell population of metabolically active cells was observed by emission of green fluorescence. This study has shown positive results for all formulations, as live cells were seen within the hydrogels up to 72 h of culturing. However, these viability experiments did not enable us to conclude on the cellular adhesion to the material and cellular proliferation.

In this work, we have proposed the use of GG hydrogel matrices with cell-loaded MPs as novel systems for application in NP regeneration. The combination of HAGG and LAGG had resulted in different formulations, which were investigated physicochemically and biologically. The mechanical analysis demonstrated the improvement of mechanical performance of the hydrogel matrices reinforced with 50 mg/mL of MPs. Moreover, the 25% HAGG:75% LAGG (v/v) GG hydrogel matrix is the closest substitute of NP in respect to mechanical properties. Besides the better results revealed in terms of mechanical behavior, the MPs allowed cell encapsulation and a good distribution of cells/MPs within the GG matrices. The biocompatibility studies demonstrated that the developed GG formulations were noncytotoxic over L929 cells. Moreover, the *in vitro* cell encapsulation studies revealed that L929 cells encapsulated in the GG MPs/hydrogel matrices remained viable for 72 h. As a final remark, the GG hydrogel matrices reinforced with cell-loaded MPs appears to be a suitable strategy for developing injectable substitutes for the efficient regeneration of NP.

Acknowledgments

The authors would like to acknowledge the Portuguese Foundation for Science and Technology (FCT) through the POCTI and FEDER programs, including Project ProteoLight (Grant No. PTDC/FIS/68517/2006) for the provided funds. This work was also carried out under the scope of European Union–funded Collaborative Project Disc Regeneration (Grant No. NMP3-LA-2008–213904).

Disclosure Statement

No competing financial interests exist.

References

1. Deyo, R.A., and Weinstein, J.N. Low back pain. N Engl J Med **344,** 363, 2001.
2. Andersson, G.B. Epidemiological features of chronic low-back pain. Lancet **354,** 581, 1999.
3. Macfarlane, G.J., Thomas, E., Croft, P.R., Papageorgiou, A.C., Jayson, M.I., and Silman, A.J. Predictors of early improvement in low back pain amongst consulters to general practice: the influence of pre-morbid and episode-related factors. Pain **80,** 113, 1999.
4. Setton, L.A., Bonassar, L.J., Masuda, K., Robert, L., Robert, L., and Joseph, V. Regeneration and replacement of the intervertebral disc. In: Lanza, R.P., Langer, R., and Vacanti, J., eds. Principles of Tissue Engineering, 3rd edition. Burlington: Academic Press, 2006, pp. 877–896.
5. Shankar, H., Scarlett, J.A., and Abram, S.E. Anatomy and pathophysiology of intervertebral disc disease. Tech Reg Anesth Pain Manag **13,** 67, 2009.
6. Cassinelli, E.H., Hall, R.A., and Kang, J.D. Biochemistry of intervertebral disc degeneration and the potential for gene therapy applications. Spine J **1,** 205, 2001.
7. Bron, J.L., Helder, M.N., Meisel, H.J., Van Royen, B.J., and Smit, T.H. Repair, regenerative and supportive therapies of the annulus fibrosus: achievements and challenges. Eur Spine J **18,** 301, 2009.
8. Roughley, P.J. Biology of intervertebral disc aging and degeneration: involvement of the extracellular matrix. Spine **29,** 2691, 2004.
9. Kalson, N.S., Richardson, S., and Hoyland, J.A. Strategies for regeneration of the intervertebral disc. Regen Med **3,** 717, 2008.
10. Hurri, H., and Karppinen, J. Discogenic pain. Pain **112,** 225, 2004.
11. Woolf, A.D., and Pfleger, B. Burden of major musculoskeletal conditions. Bull World Health Organ **81,** 646, 2003.
12. Freimark, D., and Czermak, P. Cell-based regeneration of intervertebral disc defects: review and concepts. Int J Artif Organs **32,** 197, 2009.
13. Clouet, J., Vinatier, C., Merceron, C., Pot-Vaucel, M., Hamel, O., Weiss, P., Grimandi, G., and Guicheux, J. The intervertebral disc: from pathophysiology to tissue engineering. Joint Bone Spine **76,** 614, 2009.
14. Liu, Z., Jiao, Y., Wang, Y., Zhou, C., and Zhang, Z. Polysaccharides-based nanoparticles as drug delivery systems. Adv Drug Deliv Rev **60,** 1650, 2008.
15. Walker, M.H., and Anderson, D.G. Molecular basis of intervertebral disc degeneration. Spine J **4,** 158, 2004.
16. Endres, M., Abbushi, A., Thomale, U.W., Cabraja, M., Kroppenstedt, S.N., Morawietz, L., Casalis, P.A., Zenclussen, M.L., Lemke, A.J., Horn, P., Kaps, C., and Woiciechowsky, C. Intervertebral disc regeneration after implantation of a cell-free bioresorbable implant in a rabbit disc degeneration model. Biomaterials **31,** 5836, 2010.
17. Silva-Correia, J., Oliveira, J.M., Oliveira, J.T., Sousa, R.A., and Reis, R.L. Photo-crosslinked Gellangum based hydrogels: methods and uses thereof. Provisional patent (number 105030) 2010.
18. Kandel, R., Roberts, S., and Urban, J.P. Tissue engineering and the intervertebral disc: the challenges. Eur Spine J **17,** 480, 2008.

19. Chou, A.I., Reza, A.T., and Nicoll, S.B. Distinct intervertebral disc cell populations adopt similar phenotypes in three-dimensional culture. Tissue Eng Part A **14,** 2079, 2008.
20. Roughley, P., Hoemann, C., DesRosiers, E., Mwale, F., Antoniou, J., and Alini, M. The potential of chitosan-based gels containing intervertebral disc cells for nucleus pulposus supplementation. Biomaterials **27,** 388, 2006.
21. Chou, A.I., and Nicoll, S.B. Characterization of photo-crosslinked alginate hydrogels for nucleus pulposus cell encapsulation. J Biomed Mater Res A **91,** 187, 2009.
22. Chou, A.I., Akintoye, S.O., and Nicoll, S.B. Photo-cross-linked alginate hydrogels support enhanced matrix accumulation by nucleus pulposus cells in vivo. Osteoarthritis Cartilage **17,** 1377, 2009.
23. Slaughter, B.V., Khurshid, S.S., Fisher, O.Z., Khademhosseini, A., and Peppas, N.A. Hydrogels in regenerative medicine. Adv Mater **21,** 3307, 2009.
24. Baer, A.E., Wang, J.Y., Kraus, V.B., and Setton, L.A. Collagen gene expression and mechanical properties of intervertebral disc cell–alginate cultures. J Orthop Res **19,** 2, 2001.
25. Vernengo, J., Fussell, G.W., Smith, N.G., and Lowman, A.M. Evaluation of novel injectable hydrogels for nucleus pulposus replacement. J Biomed Mater Res B Appl Biomater **84,** 64, 2008.
26. Halloran, D.O., Grad, S., Stoddart, M., Dockery, P., Alini, M., and Pandit, A.S. An injectable cross-linked scaffold for nucleus pulposus regeneration. Biomaterials **29,** 438, 2008.
27. Calderon, L., Collin, E., Velasco-Bayon, D., Murphy, M., O'Halloran, D., and Pandit, A. Type II collagen-hyaluronan hydrogel-a step towards a scaffold for intervertebral disc tissue engineering. Eur Cell Mater **20,** 134, 2010.
28. Silva-Correia, J., Oliveira, J.M., Caridade, S.G., Oliveira, J.T., Sousa, R.A., and Reis, R.L. Gellan gum-based hydrogels for intervertebral disc tissue engineering applications. J Tissue Eng Regen Med **5,** e97, 2011.
29. Bertram, H., Kroeber, M., Wang, H., Unglaub, F., Guehring, T., Carstens, C., and Richter, W. Matrix-assisted cell transfer for intervertebral disc cell therapy. Biochem Biophys Res Commun **331,** 1185, 2005.
30. Sawamura, K., Ikeda, T., Nagae, M., Okamoto, S., Mikami, Y., Hase, H., Ikoma, K., Yamada, T., Sakamoto, H., Matsuda, K., Tabata, Y., Kawata, M., and Kubo, T. Characterization of in vivo effects of platelet-rich plasma and biodegradable gelatin hydrogel microspheres on degenerated intervertebral discs. Tissue Eng Part A **15,** 3719, 2009.
31. Oliveira, J.T., Santos, T.C., Martins, L., Silva, M.A., Marques, A.P., Castro, A.G., Neves, N.M., and Reis, R.L. Performance of new gellan gum hydrogels combined with human articular chondrocytes for cartilage regeneration when subcutaneously implanted in nude mice. J Tissue Eng Regen Med **3,** 493, 2010.
32. Oliveira, J.T., Santos, T.C., Martins, L., Picciochi, R., Marques, A.P., Castro, A.G., Neves, N.M., Mano, J.F., and Reis, R.L. Gellan gum injectable hydrogels for cartilage tissue engineering applications: in vitro studies and preliminary in vivo evaluation. Tissue Eng Part A **16,** 343, 2010.
33. Oliveira, J.T., Martins, L., Picciochi, R., Malafaya, P.B., Sousa, R.A., Neves, N.M., Mano, J.F., and Reis, R.L. Gellan gum: a new biomaterial for cartilage tissue engineering applications. J Biomed Mater Res Part A **93,** 852, 2010.
34. Moorhouse, R., Colegrove, G.T., Sandford, P.A., Baird, J.K., and Kang, K.S. A New gel-forming polysaccharide. In: Brandt, D.A., ed. PS-60: Solution Properties of Polysaccharide. Washinghton, DC: American Chemical Society, 1981, pp. 111–124.
35. Hennink, W.E., and van Nostrum, C.F. Novel crosslinking methods to design hydrogels. Adv Drug Deliv Rev **54,** 13, 2002.
36. Coviello, T., Matricardi, P., Marianecci, C., and Alhaique, F. Polysaccharide hydrogels for modified release formulations. J Control Release **119,** 5, 2007.
37. Ohtsuka, A., and Watanabe, T. The network structure of gellan gum hydrogels based on the structural parameters by the analysis of the restricted diffusion of water. Carbohydr Polym **30,** 135, 1996.
38. Hamcerencu, M., Desbrieres, J., Khoukh, A., Popa, M., and Riess, G. Synthesis and characterization of new unsaturated esters of Gellan gum. Carbohydr Polym **71,** 92, 2008.
39. Basmanav, F.B., Kose, G.T., and Hasirci, V. Sequential growth factor delivery from complexed microspheres for bone tissue engineering. Biomaterials **29,** 4195, 2008.
40. Yu, J., Du, K.T., Fang, Q., Gu, Y., Mihardja, S.S., Sievers, R.E., Wu, J.C., and Lee, R.J. The use of human mesenchymal stem cells encapsulated in RGD modified alginate microspheres in the repair of myocardial infarction in the rat. Biomaterials **31,** 7012, 2010.
41. Sudhamani, S.R., Prasad, M.S., and Sankar, U.K. DSC and FTIR studies on Gellan and Polyvinyl alcohol (PVA) blend films. Food Hydrocolloids **17,** 245, 2003.
42. ISO/EN10993–5. Biological Evaluation of Medical Devices—Part 5: Tests for Cytotoxicity: In Vitro Methods. Geneva, Switzerland: International Standards, 1992.
43. Salgado, A.J., Coutinho, O.P., and Reis, R.L. Novel starch-based scaffolds for bone tissue engineering: cytotoxicity, cell culture, and protein expression. Tissue Eng **10,** 465, 2004.
44. Haugland, R.P. Handbook of Fluorescent Probes and Research Chemicals, 7th edition. Eugene, OR: Molecular Probes Inc., 1999.
45. Tako, M., Teruya, T., Tamaki, Y., and Konishi, T. Molecular origin for rheological characteristics of native gellan gum. Colloid Polym Sci **287,** 1445, 2009.
46. Holmes, A.D., and Hukins, D.W. Analysis of load-relaxation in compressed segments of lumbar spine. Med Eng Phys **18,** 99, 1996.
47. Leahy, J.C., and Hukins, D.W. Viscoelastic properties of the nucleus pulposus of the intervertebral disk in compression. J Mater Sci Mater Med **12,** 689, 2001.

Address correspondence to:
Diana Ribeiro Pereira, M.Sc.
3B's Research Group—Biomaterials,
Biodegradables and Biomimetic
Headquarters of the European Institute of Excellence
on Tissue Engineering and Regenerative Medicine
University of Minho
AvePark
S. Cláudio de Barco
4806-909 Guimarães
Portugal

E-mail: drppimenta@gmail.com

Received: February 23, 2011
Accepted: May 16, 2011
Online Publication Date: July 6, 2011